

The University of Maine

DigitalCommons@UMaine

---

Honors College

---

Winter 12-2016

## Citrate's Counter Ions and pH Effect on Gold Nanoparticle Growth Kinetics

Andrew B. Closson  
*University of Maine*

Follow this and additional works at: <https://digitalcommons.library.umaine.edu/honors>



Part of the [Biological Engineering Commons](#)

---

### Recommended Citation

Closson, Andrew B., "Citrate's Counter Ions and pH Effect on Gold Nanoparticle Growth Kinetics" (2016).  
*Honors College*. 374.

<https://digitalcommons.library.umaine.edu/honors/374>

This Honors Thesis is brought to you for free and open access by DigitalCommons@UMaine. It has been accepted for inclusion in Honors College by an authorized administrator of DigitalCommons@UMaine. For more information, please contact [um.library.technical.services@maine.edu](mailto:um.library.technical.services@maine.edu).

CITRATE'S COUNTER IONS AND PH EFFECT ON GOLD NANOPARTICLE  
GROWTH KINETICS

by

Andrew B. Closson

A Thesis Submitted in Partial Fulfillment of the Requirements for a Degree with Honors  
(Bioengineering)

The Honors College

University of Maine

December 2016

Advisory Committee:

Michael D. Mason, Professor of Chemical and Biological Engineering, Advisor

Michael Atkinson, Scientist, IDEXX Laboratories

Rosemary Smith, Professor of Electrical and Computer Engineering

William DeSisto, Professor of Chemical and Biological Engineering

François G. Amar, Professor of Chemistry and Dean of the Honors College

## Abstract

The effects of citrate's counterions and pH are examined in gold nanoparticle growth kinetics. The growth of gold nanoparticles from citrate reduction is a common method used for creating particles from 10-120 nm with a well-defined size distribution [1-4]. TEM observation of the seed-mediated growth shows an intermediate aggregation phase that has been shown by researchers to exist in other solution-phase nanocrystal growth [5]. We have shown that this intermediate agglomeration phase within particle growth may be avoided with certain pairings of counterion and pH. This aggregation phase has no noticeable effects on the formation of the particles at a smaller scale but may be cause for concern when the seed-mediated growth process is used at higher particle concentration and larger volumes. The ability to get rid of this aggregation phase at a small scale may help avoid unwanted particle characteristics at an industrial scale which includes increased volume and concentration of production.

## Acknowledgements

I would like to thank IDEXX Laboratories, specifically the Rare Reagent Design and Development group, for their help and generosity. I would also like to thank Dr. Michael Mason for his guidance.

## Table of Contents

Title Page .....	i
Abstract .....	ii
Acknowledgements.....	iii
Table of Contents.....	iv
List of Figures .....	v
Background.....	1
Introduction.....	6
Materials and Methods.....	8
Results and Discussion .....	15
Conclusion .....	27
Bibliography .....	28
Appendix A.....	30
Author's Biography .....	32

## List of Figures

Figure 1: Seed-mediated Growth Schematic .....	3
Figure 2: Front and Cross Section Views of the Analytical Disc Centrifuge.....	10
Figure 3: Initial Display of Disc Centrifuge .....	11
Figure 4: Overlaid Time Series Data .....	12
Figure 5: Size and Distribution Data Manipulated to a Single Point.....	14
Figure 6: Growth Step of Seed Mediated Particle Growth.....	15
Figure 7: TEM Images of Intermediate Aggregation During Growth Step.....	17
Figure 8: Comparing Different Citrate Counterions as Reducing Agents.....	19
Figure 9: Citrate's Three Counterions and %growth.....	21
Figure 10: Comparing Gold Chloride's Counterions at pH 7.3.....	23
Figure 11: pH Changes for Each Counterion.....	24
Figure 12: Aggregation Changes at Each pH .....	26
Figure 13: Comparing Gold Chloride's Counterions at pH 6.7 .....	Appendix A

Equation 1-3: Reduction of Gold Chloride.....	3
Equation 4: Solving for Weighted Diameter .....	14
Equation 5: Solving for Standard Deviation.....	14
Equation 6: Solving for $D_w/\sigma^2$ .....	14

## Background

One of the more exciting fields of science that has developed in the last few decades is nanotechnology. Nanotechnology has led to advances in electronics, imaging, medicine, agriculture, and much more [6-8]. To fully understand topics in nanotechnology one must first understand what the nanoscale means. Typically the nanoscale is a length scale between 1-100 nanometers. A single nanometer is a thousand times smaller than a micrometer or a billion times smaller than a meter. This is almost unfathomably small, much smaller than the human eye can see. It is approximately 10,000 times smaller than the width of a human hair.

What makes the nanoscale interesting for scientific purposes is that at such a small scale compounds that have well defined properties, such as melting points and electrical conductivities, see changes. Much of these changes are due to the change in relative surface area to volume ratio of the particles. If you imagine a cubic particle that is a length of 1 centimeter, it has a volume of  $1\text{cm}^3$  and a surface area of  $6\text{cm}^2$ . Now if you imagine that cubic particle is cut up into many smaller cubic particles 1nm in length, the total volume would be the same  $1\text{cm}^3$  however now the total surface area of all the particles would be  $60,000,000\text{cm}^2$  [9]. This massive increase in surface area is what leads to many of these interesting properties. The unique properties that emerge at the nanoscale such as changes in electrical conductivity and chemical reactivity allow nanoparticles to have many practical uses. For example gold nanoparticles are not the characteristic yellow color of bulk gold but either a red or purple color based on their size. This change in optical properties with particle size offers many benefits in optical

instrumentation and diagnostics. Along with size-related electronic and optical properties nanoparticles can have applications in catalysis [10].

The use of nanoparticles in art has been around since the Roman times. The Lycurgus Cup is a chalice crafted in the ancient Roman Empire, 1,600 years ago, that shows interesting properties because its glass is impregnated with gold nanoparticles [11]. The gold nanoparticles cause changes in the color of the cup depending on the light source. Light transmitted through the cup, from the inside, makes the cup appear a ruby red color while light from the outside of the cup reflects off the cup causing it to appear green [10]. In the 1850's Michael Faraday was the first to produce an aqueous solution of gold nanoparticles by reducing a solution of chloroaurate with phosphorus [10]. Through the late 1900s many different processes for creating gold nanoparticles were devised. The most commonly used aqueous synthesis of gold nanoparticles was first described by Turkevich et al. as a reduction of chlorauric acid by sodium citrate [2]. The sodium citrate also acts as a capping agent which stabilizes the formed nanoparticles [12]. This synthesis was later refined by Frens to include accurate size targeting of particles with varying reagent concentrations [13].

The spherical gold nanoparticle synthesis that we will be focusing on is the classic Turkevich method. A gold hydrochlorate solution is reduced by sodium citrate causing the solution to change from yellow to clear and then to dark blue and finally to a red wine color [2, 13, 14]. Equations 1-3 show the reduction of gold chloride by sodium citrate, producing the neutral gold atom. The gold zero collides with one another, known as nucleation, and creates small particles. More gold zero can now start to either collide with the formed gold particles, creating larger particles or continue to collide with one another

forming more nucleation events. The relative rates of both events depend on concentration of reagents and time.

Equations 1-3: Reduction of gold chloride by sodium citrate

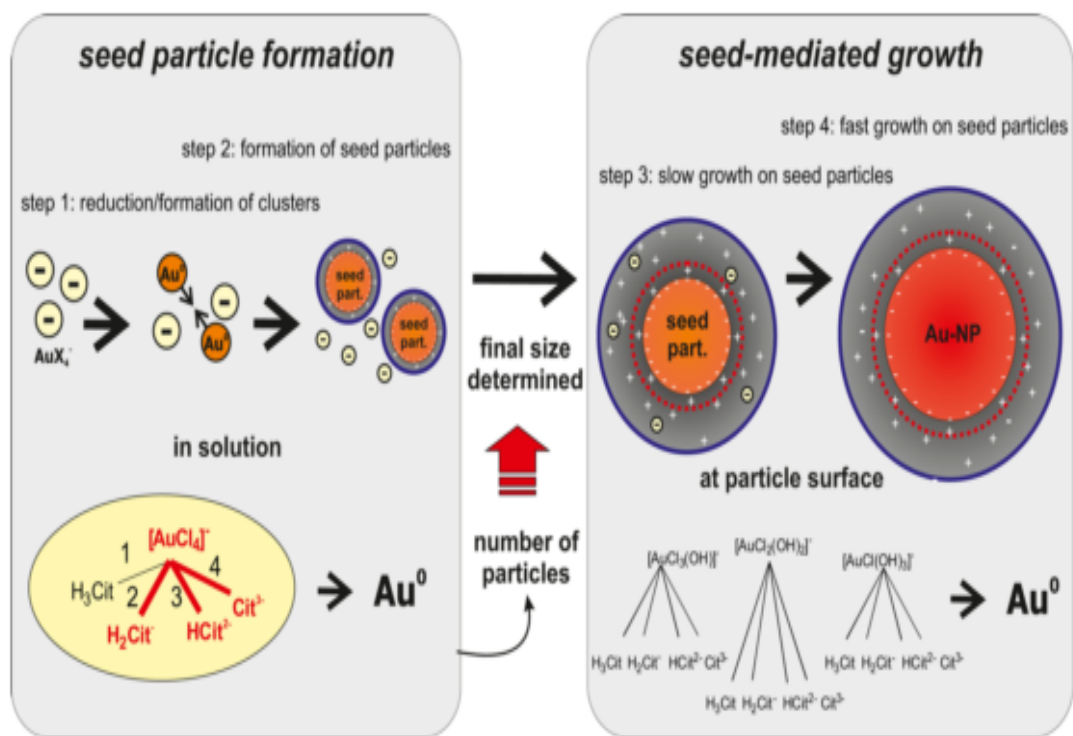
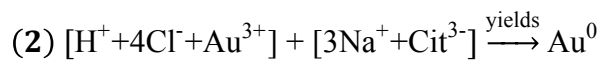


**Figure 1:** Seed-mediated growth schematic, showing the formation of  $\text{Au}^0$  from the reduction of gold ions, the formation of nucleation sites from  $\text{Au}^0$  collision, and the growth of seeds to larger particles. Schematic taken from Kettemann et. al. [4].

The process of first creating smaller “seed” particles and then subsequently growing them larger and larger over a period of “growth steps” is known as seed-mediated growth. After each growth step the reaction is allowed to sit at temperature for 15 minutes before proceeding. This has been shown to allow for a more complete separation of particles from the nanowires originally formed [12]. A schematic representing nanoparticle growth from reagents to seeds to large particles can be seen in Figure 1.

By utilizing seed-mediated growth and the Turkevich method, gold nanoparticle seeds are created and as more gold chloride is added during each growth step, the particles can be grown to specific sizes. A benefit of a seed-mediated growth is that it has been shown to allow for more uniform growth of particles [15]. Seed-mediated growth also gives benefits in reducing secondary nucleation events that occur and appear in the size distribution data [10]. It has been shown to be able to produce particles from 15-300nm particles [1].

This study is most interested in the reducing agent, sodium citrate, and the dark blue color change that occurs during seed synthesis and how a similar effect might take place during each growth step of seed mediated growth. The dark blue stage of synthesis has been shown to be made up of gold nanowires interconnected in an extensive network [12]. This network will later fragment into spherical particles. During seed-mediated growth the intermediate aggregation state mentioned later is most likely related to this darkening stage during synthesis.

When trying to push concentration of particles being synthesized it can be assumed that since aggregation events can cause colloidal instability, avoiding any intermediate aggregation states during particle growth could lead to the production of higher

concentrated gold spheres. For future industrial scaled production of gold nanoparticles it is beneficial to produce higher concentrations of particles as this limits the volume needed to produce the same number of particles. At large scale, 100 liters of a concentration of gold could be replaced by 10 liters of gold at 10X the concentration. This significantly reduces production and storage size. At the same time there are many foreseen benefits of a narrowly distributed nanoparticle. Specific optical resonance in the visible range is sensitive to size of the particles so maintaining a well-defined uniform size would be beneficial [16, 17]. Balancing these two is what has led to the interest in the reaction parameters of the reducing agent and pH.

## Introduction

Nanoparticles are undoubtedly a critical component of many of today's advancements in science and medical technology. Specifically, synthesis and applications of gold nanoparticles (AuNP) have been studied extensively for decades. Researchers have been studying the mechanism of AuNP synthesis since 1951, when Turkevich et. al. developed a synthesis procedure centered around the reduction of tetrachloroauric acid by sodium citrate [2]. This synthesis was later refined by Frens et. al. [13]. While this synthesis is known as the "gold" standard today, other synthesis procedures have been developed and are also widely used. More recent efforts have been focused more heavily on increasing monodispersity and shape/size control with various synthesis methods. However, the practical applications of gold nanoparticles are limited by a lack of ability to scale up the synthesis while maintaining a high product quality. Lower quality products can cause issues during surface modifications.

Early work in gold nanoparticles identifies color changes in solution during the synthesis process [2]. The yellow color provided by tetrachloroauric acid quickly disappears once the reduction begins and gives way to a very dark blue solution. Once the reduction has reached completion, the colloid solution reaches its final characteristic deep red color. This dark blue stage during synthesis has been characterized and shown to consist of a network of nanorods [12]. We believe a similar transition state occurs during seed-mediated particle growth and we will characterize it by showing nanoparticle morphology with transmission electron microscopy and analytical disc centrifugation. These techniques will make the case that by adjusting reaction parameters the resulting nanoparticles will have reduced aggregation during their growth steps. Avoiding the

intermediate aggregation state of gold nanoparticle growth will result in more monodisperse particles that are higher in quality and more conducive to being used for technical and medical applications requiring a higher degree of precision and process control.

Herein, we describe for the first time an approach for gold nanoparticle seed-mediated growth where we carefully monitor the size of the particles during the time following  $\text{HAuCl}_4$  addition. By monitoring the size of the particles over time with an analytical disc centrifuge, an intermediate aggregation state is seen that gave cause for concern in the purity of an industrial scaled production. We attempt to make use of hard and soft ions electronegativity (HSAB Theory) and pH control to eliminate the presence of this intermediate aggregation state.

By looking at an ion series for the reducing agent citrate, we were able to make use of the hard and soft ions to control the presence of the intermediate aggregation state. It is commonplace in academia and industry to use sodium citrate as a reducing agent for the production of gold nanoparticles. Using potassium, sodium and lithium citrate, changes in cation electronegativity led to varying levels of intermediate aggregation of particles. A decrease in pH led to similar improvements by minimizing intermediate aggregation. This is promising for industrial scale reactions as it provides a cheaper way to improve particle growth compared to the more expensive lithium citrate.

## Materials and Methods

### Seed Synthesis

Gold nanoparticle seeds were synthesized in 100mL batches using citrate reduction of aqueous gold chloride. 96mL of Deionized (DI) water was heated to 90 °C and spun with a magnetic stir bar at approximately 540rpm, or until a small vortex was formed.  $\text{HAuCl}_4$  from Sigma-Aldrich was used to form a solution in water that contained 0.7mM of gold atoms. 1mL of this solution was added to the reaction vessel and allowed to mix thoroughly. Lithium, Sodium, and Potassium Citrate from Sigma-Aldrich were formed into their respective 1M stock solutions. These stock solutions were analyzed with High Performance Liquid Chromatography (HPLC) to determine their citrate content. This allowed for the normalizations of the three solutions to their citrate contents. These 1M solutions were diluted in DI water to create solutions that had a relative citrate concentration of 7mM. 3mL of one of these solutions, depending on the experiment trial, was then added to the reaction vessel. The reaction was run for 3 hours before being allowed to cool to room temperature. Glassware was cleaned using concentrated aqua regia, which is a 3:1 ratio of concentrated HCl to Nitric Acid. Aqua regia is able to dissolve noble metals such as platinum and gold. By cleaning with the glassware with it, we were certain that each experiment began with glassware containing no gold, which could act as nucleation sites for the formation of undesired particles.

### Particle Growth

Seeds synthesized with Lithium Citrate in previous reactions had their pH's adjusted to either 6.7 or 7.3 using dilute Lithium Hydroxide from Sigma-Aldrich.

Likewise seeds synthesized with Sodium Citrate and Potassium Citrate had their pH's adjusted using Sodium Hydroxide and Potassium Hydroxide from Sigma-Aldrich, respectively. These solutions were then heated to 90 °C and spun at 540 rpm or until a small vortex was formed. Solutions of  $\text{HAuCl}_4$ ,  $\text{LiAuCl}_4$ ,  $\text{NaAuCl}_4$ , and  $\text{KAuCl}_4$  from Sigma-Aldrich were made to each contain a concentration of 0.175mM gold atoms. To start the growth step and begin taking samples, 1mL of one of the gold chloride solutions is added to the reactions.  $\text{LiAuCl}_4$  was only added to reactions synthesized with Lithium Citrate,  $\text{NaAuCl}_4$  was only added to reactions synthesized with Sodium Citrate, and  $\text{KAuCl}_4$  was only added to reactions synthesized with Potassium Citrate. While  $\text{HAuCl}_4$  was added to reactions synthesized with all three types of citrate. After 15 minutes the growth step was considered to be done and the reaction was removed from heat and allowed to cool to room temperature.

### Analytical Disc Centrifuge

An analytical disc centrifuge is a powerful analytical tool that measures particle size and distribution. It operates using centrifugal sedimentation in a liquid medium. An optically clear disc is filled with a liquid gradient and spun at high speeds. Particles are injected into the center of the rotating disc and sediment to the outside of the disc based on their size. A light beam on the edge of the disc records when particles block its path and converts the time it takes for these particles to arrive at the light beam to particle size. By varying the liquid gradient and disc rotation speed, a large size range of particles can be analyzed. The specific instrument we used offers a range from 2nm to 80  $\mu\text{m}$ .

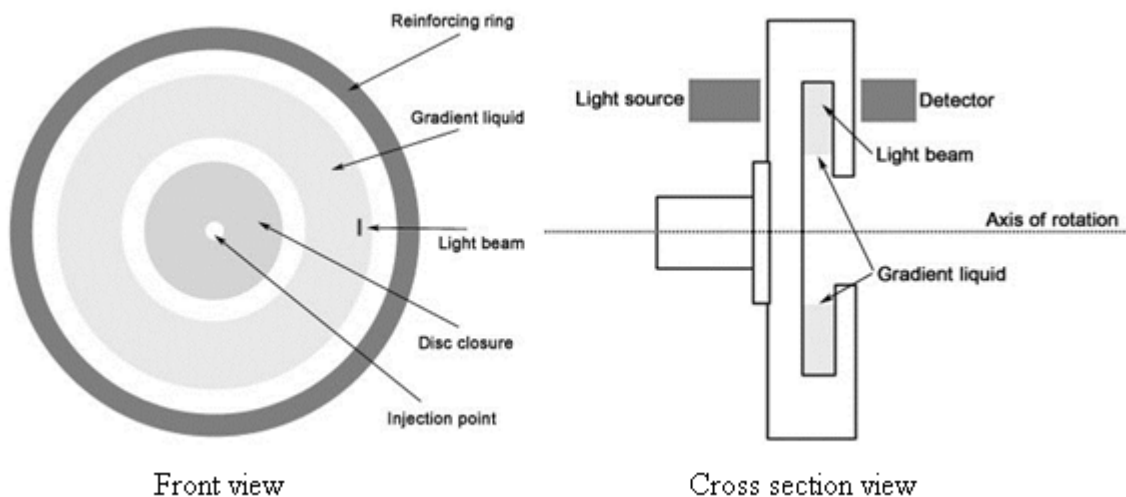


Figure 2: The front and cross section views of the CPS Instruments Disc Centrifuge UHR. Injection points, gradient liquid and light beam paths can be seen at both viewing angles. When injected, particles are forced to the outside of the ring at varying rates based on size. The time it takes for particles to block the light beam is related to particle size using algorithms within the instrument. Images were taken from CPS Instruments website.

A CPS Instruments Disc Centrifuge UHR was used for the analysis of particle size. A 12mL sucrose gradient was used from 8-24 weight/weight%. It was calibrated at 40nm using 40nm gold particles from BBI Solutions. 1mL samples were taken directly from reactions and cooled on ice at specific time points. 100 $\mu$ L samples were shot, undiluted into the instrument for analysis. Samples were taken before the growth step began and at 30, 60, 120, 300 and 900 seconds afterwards. Data from the disc centrifuge is initially represented in a plot of the Relative Weight vs Particle Diameter in microns. Other information available on the display includes the width of the curve at 10% of the peak height, which can be used as a distribution measurement, and percent weights in different ranges of particle size. This initial display is useful in first analyzing the quality of the product. It is easy to see when problems occur by looking at measured peak size and shape against expected values.

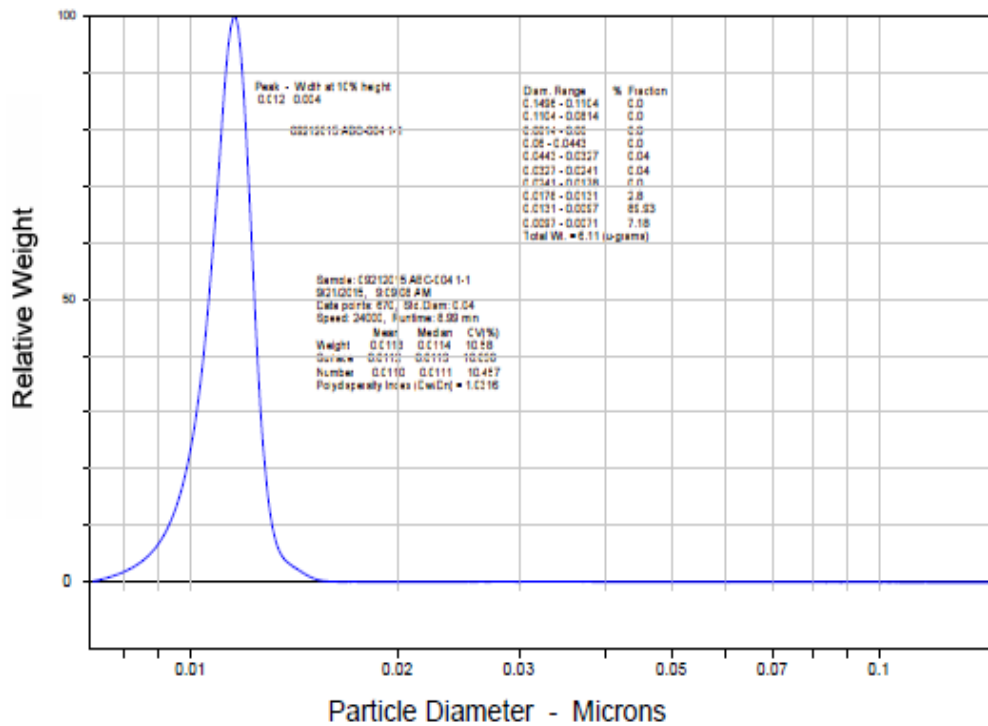


Figure 3: An example of the disc centrifuge's display of particle size after seed synthesis. The particles can be easily seen to be around 12nm and have a width at 10% of the max height of 4nm. This viewing screen offers a quick and easy way to check particle sizes and distribution.

The display settings on the disc centrifuge also allow for the overlaying of previously analyzed particles. This allows for a visual comparison of particle size and distribution. An example of this can be seen below. Where the three curves are three separate particles measured. Here we can see a comparison of particles at various time points along a particle growth step.

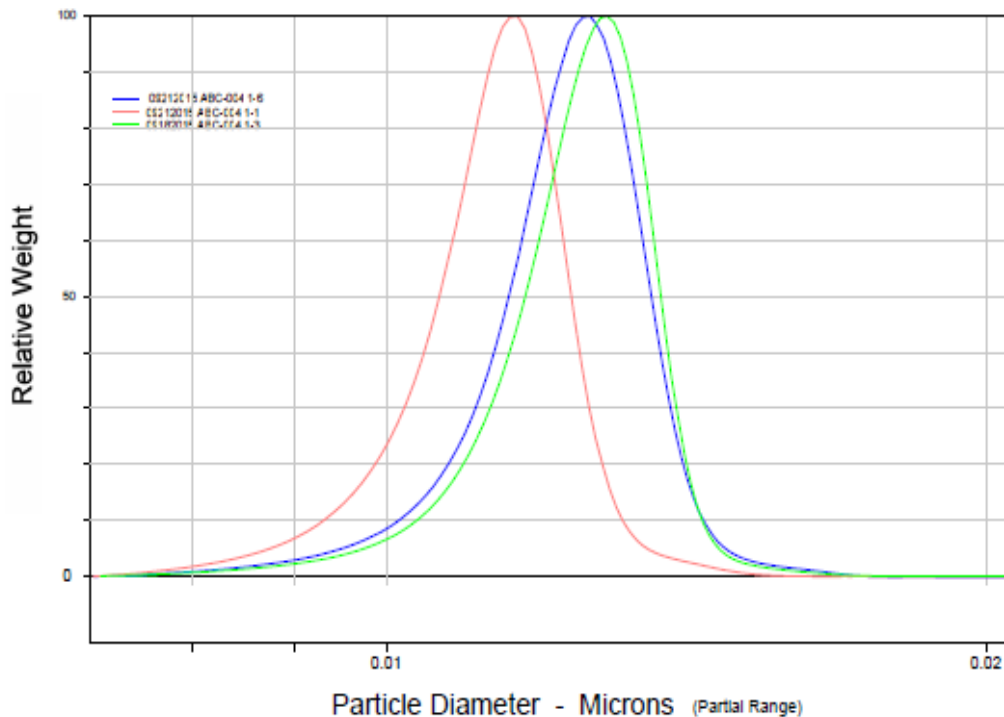


Figure 4: Disc Centrifuge display of an overlay of 3 different measurements. The red plot represents the start of particle growth, the green plot is 30 seconds into particle growth and the blue plot is at the end of particle growth. It can be seen here that during the intermediate stages of growth, particles first have larger size distributions and apparent sizes then lower to their final size.

### Data Analysis

The disc centrifuge offers more tabulated data than what is displayed when collecting samples. Each sample run gives various measurements including diameter and peak height based on weight, surface, number or absorbance. In this paper we made use of the height data by weight and diameter. To better analyze the time series data that we created we needed a method to summarize each time point's data set in a single data point. To do this we manipulated the diameter associated with each data point of the

relative weights to create a weight weighted average diameter/ standard deviation. Equations 4, 5, and 6 were used in order to produce this new value, they are all listed below. This gave a single data point that represented both the average diameter of the particle at the given time point and its size distribution. In the figure below the entire data set for a distribution taken 30 seconds into a growth step is seen in part A. In part B of the figure the single data point highlighted in the time series plot represents the previous data set as a relation between the average diameter and the curves distribution.

Time series data sets like those above were compared to each other with various parameters including pH and citrate counter ion. Along with these weighted average diameters, growth percent changes in diameter were also plotted to give slightly different representations of each time series.

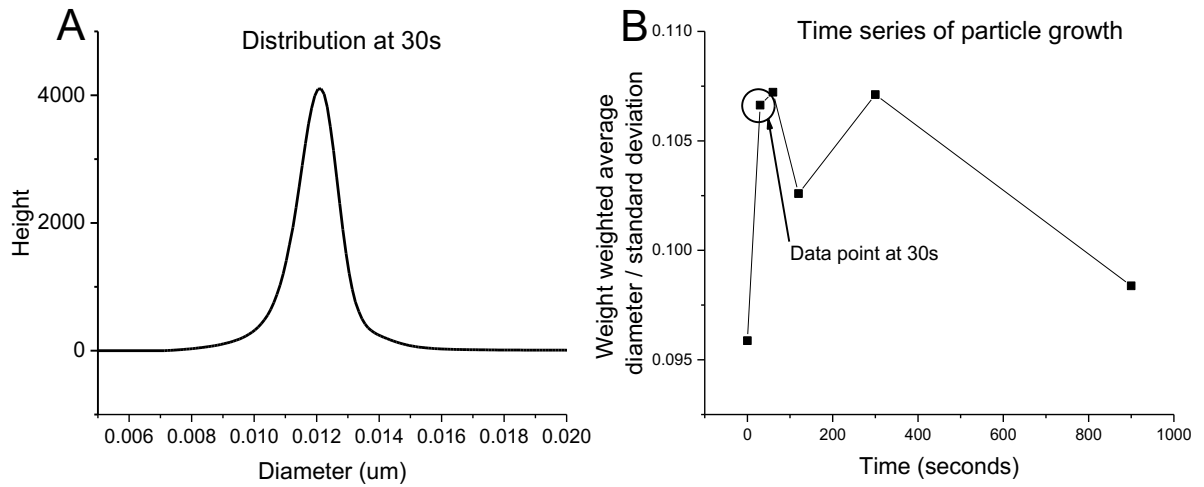


Figure 5: Section A shows a distribution of weights vs. diameter of particles 30 seconds into a growth step. Section B shows the entire time series data focused in to a single plot. Each data point represents the size and distribution at a given time point during growth. The 30 second time point is highlighted to show its relation to section A.

Equation (4) 
$$D_w = \frac{\sum D_i * W_j}{\sum W_j}$$

Equation (5) 
$$\sigma^2 = \frac{\sum [(D_i - D_w)^2 * (\frac{W_j}{D_i^2})]}{\sum (D_i - D_w)^2}$$

Equation (6) 
$$\frac{\text{weight weighted average diameter}}{\text{standard deviation}} = \sqrt{\frac{\sigma^2}{D_w}}$$

## Results and Discussion

### Intermediate aggregation during particle growth

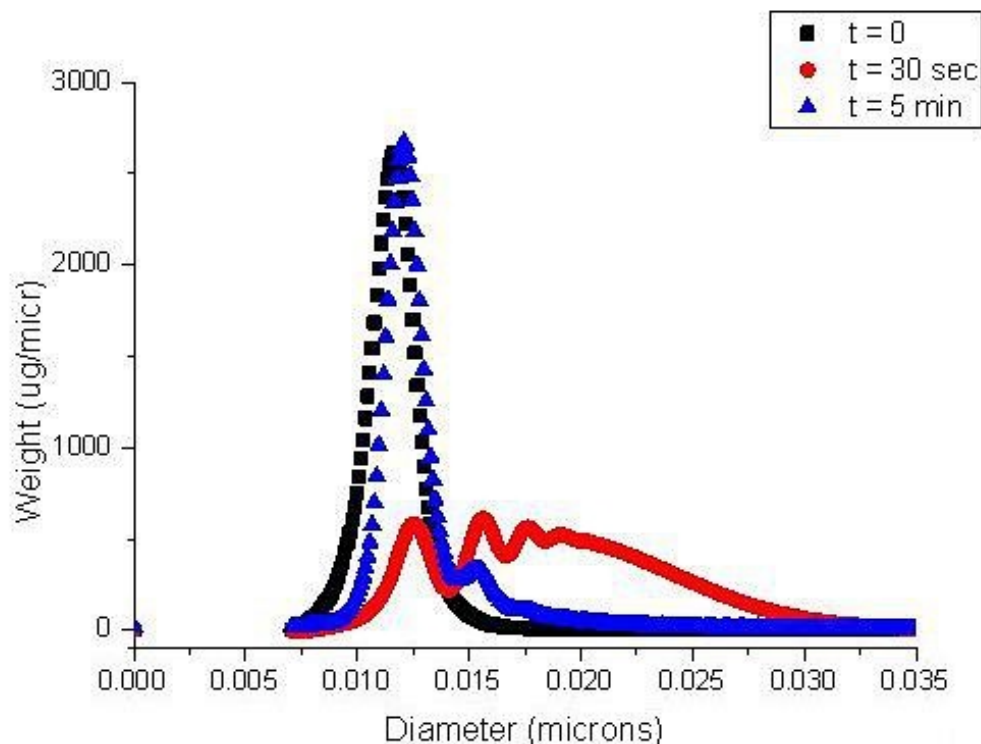


Figure 6: Weight distributions as a function of particle diameter from disc centrifuge analysis of seeded sodium citrate Au NP growth at indicated time points. The three time points represented are the initial seeds ( $t = 0$ ) and intermediates ( $t = 30$  sec,  $t = 5$  min) of seeded growth.  $t = 0$  corresponds to a sample taken before the start of a growth step,  $t = 30$  sec corresponds to a sample taken 30 seconds into the growth step and  $t = 5$  min corresponds to a sample taken 5 minutes into the growth step. Multimodal distribution is clearly visible for the 30-second intermediate. Weight distribution is unimodal at  $t = 0$  (before starting growth) and slightly bimodal at  $t = 5$  min (at which point, a single growth step with one addition of gold is complete). Bimodal weight distribution at  $t = 5$  min may indicate aggregation or secondary nucleation.

In the classic Turkevich method gold nanoparticle synthesis sodium citrate reduces  $\text{Au}^{3+}$  ions from gold chloride [2, 13, 14]. Upon addition of sodium citrate to a gold hydrochlorate solution the color of the solution changes from yellow to clear and then again to a dark blue and finally a red wine color characteristic of 10-20nm gold nanoparticles. The dark blue intermediate color transition has been investigated by others

and shown to be an aggregation state of an extensive network of gold nanowires [12]. Upon their synthesis, gold nanoparticles can be subsequently grown to large sizes with the addition of more  $\text{HAuCl}_4$ . With this addition, no intermediate dark coloring is seen, but upon analysis of the solution at various time points after addition, a change in size distribution can be seen with the aid of an analytical disc centrifuge. Figure 6 shows this change. At a time point before the  $\text{HAuCl}_4$  addition a unimodal distribution is seen for the particle diameter. 30 seconds after addition a multimodal distribution is seen ranging from the original 11nm to 35nm. Following this increase in diameter distribution the final distribution is again somewhat unimodal but only a few nanometers larger than the original particles. This suggests that in a typical growth reaction there is an intermediate state similar to that of particle synthesis. This intermediate aggregation state could lead to added aggregates in samples, decreasing their particle purity.

We can compare this aggregation we see in the disc centrifuge to transmission electron microscopy images (TEM) of a typical growth of sodium citrate reduced gold seeds in Figure 7. The TEM images show severe aggregation at the one minute time point which decreases by the 15 minute time point of the typical growth step. Such an intermediate aggregation state could lead to loss of particle purity at higher particle concentrations and chemistries that require narrowly distributed particles

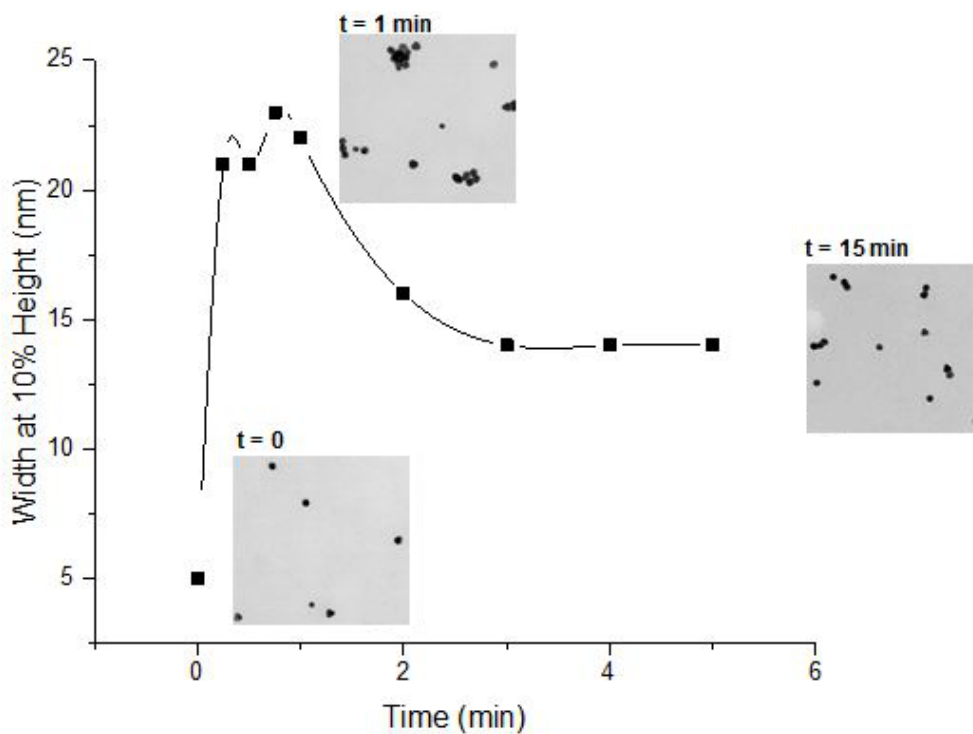


Figure 7: Size distribution (width at 10% peak height) as a function of time of seeded sodium citrate AuNP growth compared with transmission electron microscopy images of similar growth reactions over a similar time period. Spline interpolations are used for ease of visualization. Multimodal particle size distribution is clearly visible for intermediate time points and unimodal size distribution is prominent at the beginning and end of the reaction. Each TEM images in its entirety is 310nm by 297nm.

### Varying counter ion of reducing agent citrate

The effects on aggregation of surfactants with changes in counterions has been investigated by Evans et al. and has been shown to produce varying aggregation levels with simple changes in counterions [18]. Solid surfaces don't have as extreme effects from counterion changes as surfactant micelles but there should be changes nonetheless. With specific macrocyclic compounds the counter ion series of  $\text{Li}^+$ ,  $\text{Na}^+$ , and  $\text{K}^+$  showed changes in surface tension and aggregation [18]. This shows promise that changing the counterion of the reducing agent in aqueous gold nanoparticle synthesis may cause beneficial changes in terms of minimizing aggregation.

Here we investigate changes in the counter ion of the reducing agent, citrate, and its effects on the growth of gold nanoparticles. The typical reducing agent of the Turkevich method is sodium citrate, which acts as both the reducing agent and a capping agent, stabilizing the formed nanoparticles [2, 10, 12-14]. The reducing agent's counter ions we analyzed were the group 1 alkali metals lithium, sodium and potassium. Effects of the changes in ions on particle size distribution can be seen in figure 8. When sodium and potassium citrate are used as the reducing agent an intermediate aggregation phase is seen in their individual growth curves. It is with lithium citrate as the reducing agent where we see an improvement in the growth curves to a size distribution that grows over time without an intermediate aggregation phase. Figure 8 compares the three reducing agents and it can be clearly seen that growth with lithium citrate is different than with sodium and potassium citrate. The differences in growth for sodium and potassium citrate as opposed to lithium citrate can be attributed to the changes in reduction potential of the citrate with varying counter ions. The smaller lithium ions have been shown to have

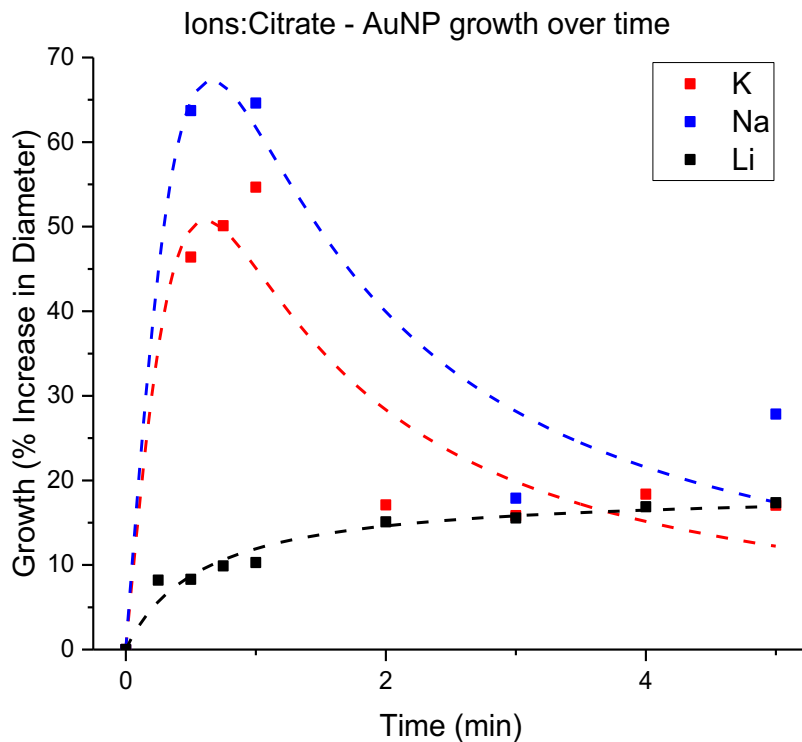


Figure 6: The three citrate counterions analyzed as reducing agents for the growth of seed - mediated gold nanoparticles were  $\text{Li}^+$ ,  $\text{Na}^+$ , and  $\text{K}^+$ . The plot compares growth as a percentage for each of the counterions. The initial increase in growth percentage seen in NaCitrate and KCitrate can be related to the large intermediate aggregation state seen previously. Interestingly when LiCitrate is used as the reducing agent, no large increase in growth percentage is seen. With lithium as the counterion the growth percentage slowly increases over time until it reaches its final size.

lower ion mobility than sodium and potassium [19]. The lower ion mobility can be attributed to resulting in a less negative reduction potential and thus produces slower rates of reaction of the citrate for reduction of  $\text{Au}^{3+}$  ions. This limits the initial burst reduction that leads to the formation of an intermediate aggregation. Assuming that these changes in reduction potential are the cause for reduced aggregation by lowering the reaction rate of citrate, we would also expect to see sodium citrate produce less aggregation than potassium citrate. However, we do not see this. Potassium citrate actually is shown to produce slightly less aggregation than sodium citrate. We attribute to the similarities in their ion mobility. The similarities allow for slight changes in ion size

and other factors to increase the relative reduction potential of sodium citrate and the gold particles as compared to potassium citrate and the gold particles. Figure 9 shows the three counter ions of citrate in their individual time series plots. Both growth percentage and normalized change in relative width are shown.

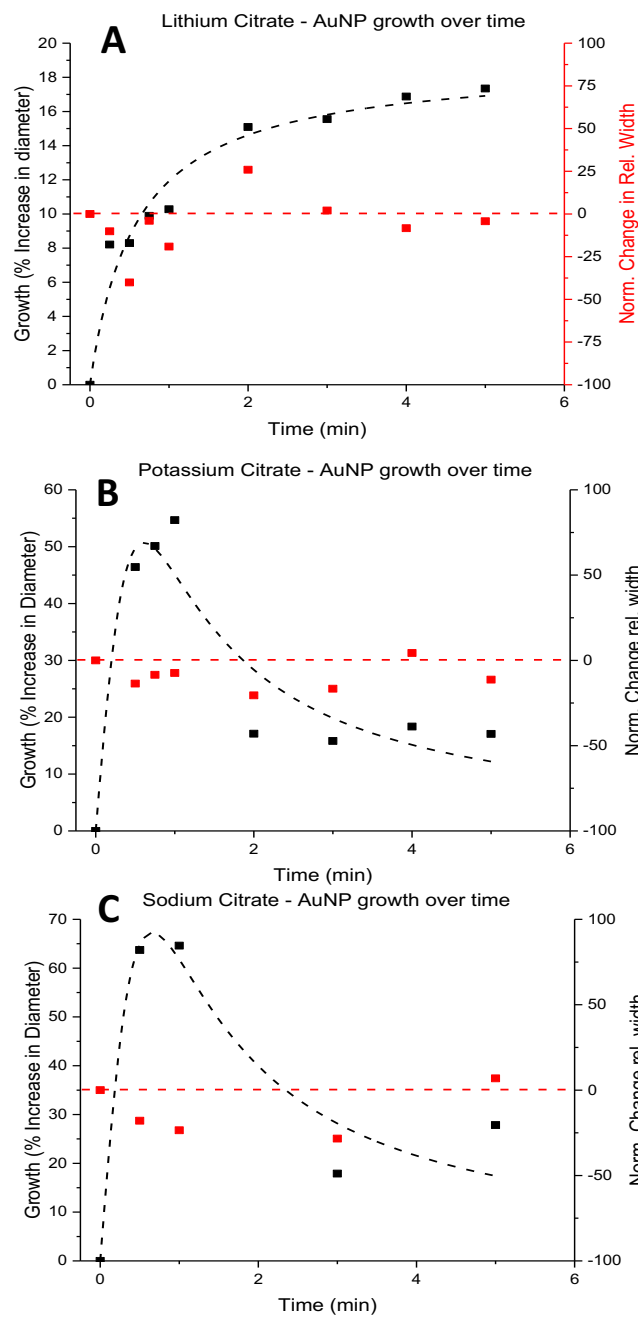


Figure 7: Viewing the three citrate counterions analyzed as reducing agents for the growth of seed-mediated gold nanoparticles,  $\text{Li}^+$ ,  $\text{Na}^+$ , and  $\text{K}^+$ , separately. Plots (A), (B), and (C) are concerned with  $\text{Li}^+$ ,  $\text{Na}^+$ , and  $\text{K}^+$  respectively. The plots show growth as a percentage increase in diameter of the particles on the left y-axis and normalized change in relative width on the right y-axis.

## Changing Counter-ion of Gold Chloride

As we analyzed different counterions of citrate so too did we analyze different counterions for gold chloride. The different gold chloride's we looked at were  $\text{HAuCl}_4$ ,  $\text{LiAuCl}_4$ ,  $\text{NaAuCl}_4$  and  $\text{KAuCl}_4$ . In each case the seeds were all synthesized using  $\text{HAuCl}_4$  with different citrates. During the growth steps is when different gold chlorides were experimented with. In Figure 10 it can be seen that in growth steps that used  $\text{LiAuCl}_4$ ,  $\text{NaAuCl}_4$  and  $\text{KAuCl}_4$  as the source of gold atoms, there was a lowering in the growth percentage as compared to  $\text{HAuCl}_4$ . We attribute this decrease in percent growth to the matching counterions of citrate and gold chloride as maximizing the relative reduction potentials. When the counterions of the reducing agent and gold chloride match, there is an increased relative reduction potential as compared to when  $\text{HAuCl}_4$  is used, decreasing the reaction rate and thus reducing the initial burst reduction that we believe leads to aggregation states.

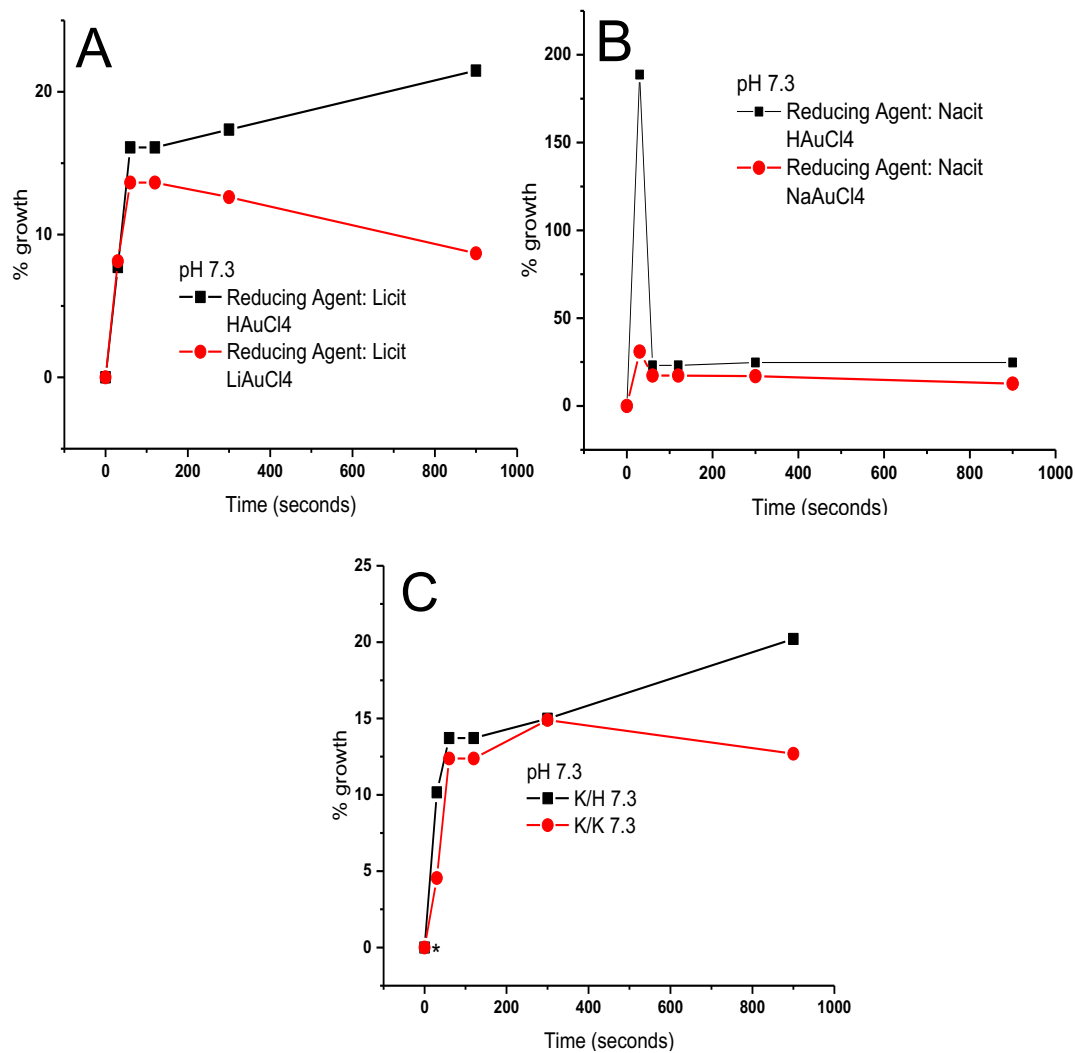


Figure 8: The three gold chloride counterions analyzed for the growth of seed-mediated gold nanoparticles were  $\text{Li}^+$ ,  $\text{Na}^+$ , and  $\text{K}^+$ . Each plot shows the comparison of  $\text{HAuCl}_4$  versus the different alkali metals as gold chloride counterions at pH 7.3. Plot (A) shows the comparison growth as a percentage for  $\text{HAuCl}_4$  and  $\text{LiAuCl}_4$ . Plot (B) shows the comparison growth as a percentage for  $\text{HAuCl}_4$  and  $\text{NaAuCl}_4$ . Plot (C) shows the comparison growth as a percentage for  $\text{HAuCl}_4$  and  $\text{KAuCl}_4$ . The plots show growth as a percentage increase in diameter of the particles versus time in seconds.

## Comparing pH for Individual Counter-ions

The standard starting pH for growth steps was a pH of 7.3, which was adjusted at the beginning of the growth step. Here we also tested a starting pH of 6.7. In figure 11 each counterion of citrate is used to reduce gold chloride at the two varying pH's. As it shows the weight weighted average diameter/standard deviation for each citrate counterion is lower at pH 6.7 when compared to 7.3. This can especially be seen with

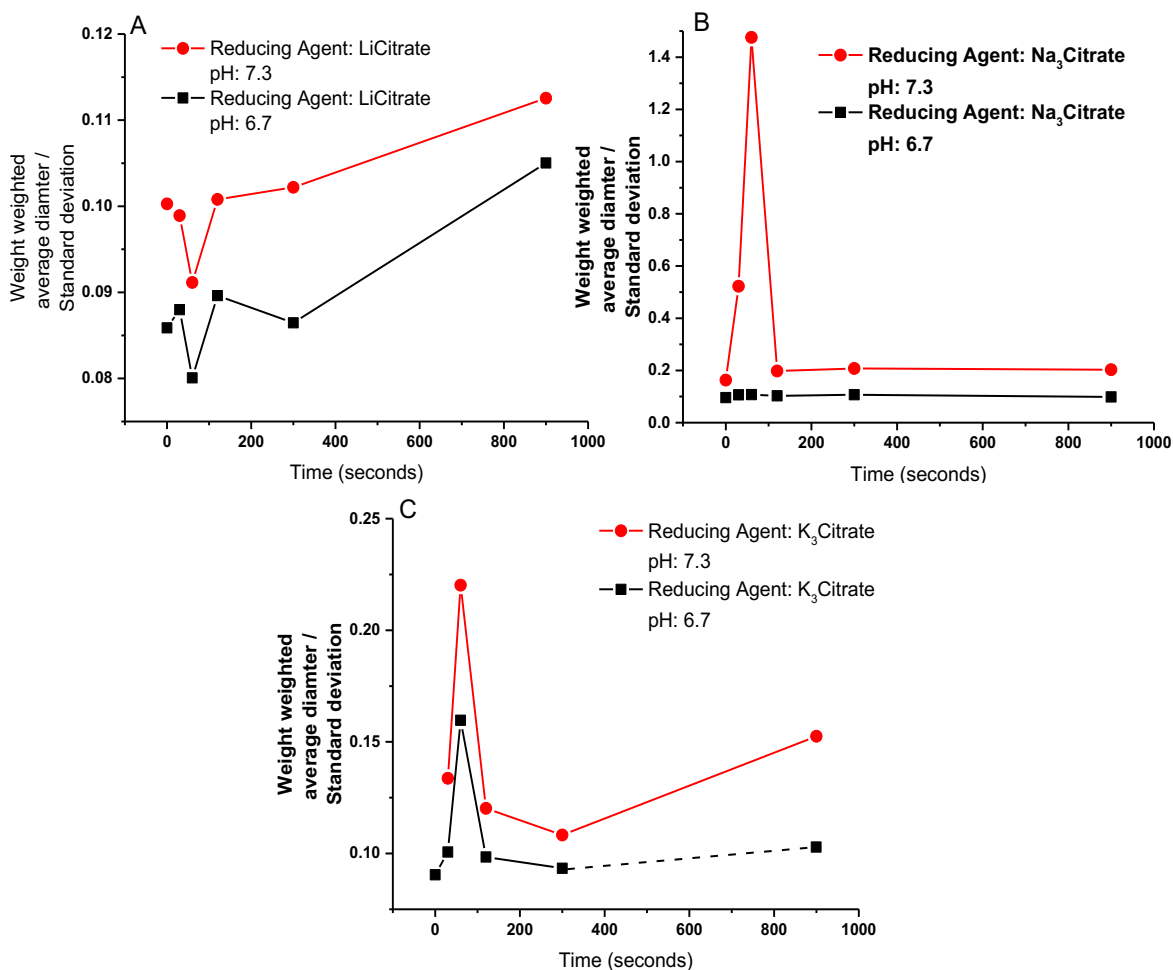


Figure 11: Comparing the weight weighted average diameter/standard deviation of gold nanoparticles synthesized at pH 6.7 and 7.3 with reducing agents lithium citrate, sodium citrate and potassium citrate. In all three cases it is seen that a lower pH decreases the size increase of the particle growth. Dotted lines show expected values of missing data. Plot (A) shows LiCitrate, Plot (B) shows NaCitrate and Plot (C) shows KCitrate.

sodium citrate reduced particles. This can be attributed to the lowering of the pH toward the 3<sup>rd</sup> pKa of citrate which changes the relative reduction potentials between the citrate and gold surface. The lower pH of 6.7 appears to decrease this relative reduction potential, slowing down the reaction and decreasing the presence of aggregates. This is most likely due to the decreased availability of citrates electrons at lower pH values.

Figure 12 shows all 3 citrate counterions at both pH 6.7 and 7.3. One interesting point here is that the citrate counterion that produces the largest intermediate aggregation state at a pH of 7.3 is sodium. While at a pH of 6.7 the largest intermediate aggregation state is caused by potassium citrate. This flip in the order of which counterion causes the most improvement in intermediate aggregation during particle growth can possibly be attributed to the relative change of reduction potential being much greater for sodium than for potassium when moving from pH 7.3 to pH 6.7, due to ion size and mobility.

Another interesting point is that reducing the pH from 7.3 to 6.7 causes the sodium citrate reduced particles to decrease their aggregation to a similar level as that of lithium citrate reduced particles. This suggests that by lowering the pH, the intermediate aggregation phase can be decreased in a similar manner to using lithium citrate as the reducing agent.

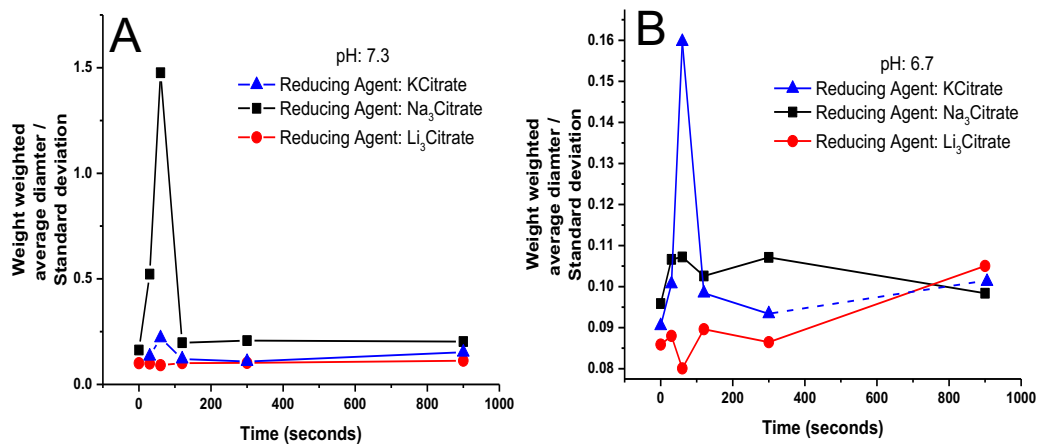


Figure 12: Plot (A) compares the 3 reducing agents of lithium, sodium and potassium citrate role in an intermediate aggregation at pH of 7.3. Plot (B) makes a similar comparison but at pH 6.7. It can be seen that when the pH is dropped to 6.7 from 7.3, the sodium citrate reduced particles produce much less aggregation.

## Conclusion

Here we have shown that an intermediate aggregation state occurs during seed mediated growth of gold nanoparticles. This intermediate aggregation state is most likely similar to the dark blue color phase seen during particle synthesis in the classic Turkevich method, which has been shown to consist of an aggregate of gold nanorods that later cleave into spheres. This intermediate aggregation state is cause for concern when considering industrial scaled production of narrowly distributed particles. We have shown here that the use of lithium citrate as the reducing agent as opposed to the conventional sodium citrate can minimize this aggregation and narrow the size distribution. Similar to the use of lithium citrate, a lowering of the starting pH before each growth step to 6.7 can reduce the aggregation state seen with sodium citrate as the reducing agent. The ability to cheaply reduce the intermediate aggregation state with pH adjustment as opposed to the more expensive use of lithium citrate offers a simple way for improved particle purity that could be useful at high particle growth concentrations, where any aggregation during the growth process could lead to problems.

## Bibliography

1. Christopher Ziegler, A.E., *Seeded Growth Synthesis of Uniform Gold Nanoparticles with Diameters of 15-300 nm*. The Journal of Physical Chemistry, 2011. **115**(11).
2. John Turkevich, P.C.S., James Hillier, *A Study of the Nucleation and Growth Processes in the Synthesis of Colloidal Gold*. 1951(11): p. 55-75.
3. Frens, G., *Particle Size and Sol Stability in Metal Colloids*. Colloid and Polymer Science, 1972. **250**(7): p. 736-741.
4. Frieder Kettemann, A.B., Steffen Witte, Maria Wuihshick, Nicola Pinna, and K.R. Ralph Kraehnert, and Jörg Polte, *Missing Piece of the Mechanism of the Turkevich Method: The Critical Role of Citrate Protonation*. Chemistry of Materials, 2016. **28**: p. 4072-4081.
5. Taylor J. Woehl, C.P., James E. Evans, Ilke Arslan, William D. Ristenpart, and a.N.D. Browning, *Direct Observation of Aggregative Nanoparticle Growth: Kinetic Modeling of the Size Distribution and Growth Rate*. Nano Letters, 2014. **14**: p. 373-378.
6. McEuen, P.L., *Nanotechnology: Carbon-based electronics*. Nature, 1998. **393**(6680): p. 15-17.
7. Otilia M. Koo, I.R., Hayat Onyuksel, *Nanomedicine: Nanotechnology, Biology and Medicine*. Nanomedicine, 2005. **1**(3): p. 193-212.
8. Rai, M. and A. Ingle, *Role of nanotechnology in agriculture with special reference to management of insect pests*. Applied Microbiology and Biotechnology, 2012. **94**(2): p. 287-293.
9. *What's So Special about the Nanoscale*. Nanotechnology 101; Available from: <http://www.nano.gov/nanotech-101/special>.
10. Daniel, M.-C. and D. Astruc, *Gold nanoparticles: assembly, supramolecular chemistry, quantum-size-related properties, and applications toward biology, catalysis, and nanotechnology*. Chemical reviews, 2004. **104**(1): p. 293-346.
11. Merali, Z., *This 1,600-Year-Old Goblet Shows that the Romans Were Nanotechnology Pioneers*, in *Smithsonian Magazine*. 2013.
12. Boon-Kin Pong, H.I.E., ‡ Jian-Xiong Chong, § Wei Ji, ‡ Bernhardt L. Trout, †, ^ and and J.-Y. Lee, *New Insights on the Nanoparticle Growth Mechanism in the Citrate Reduction of Gold(III)*

- Salt: Formation of the Au Nanowire Intermediate and Its Nonlinear Optical Properties*. Journal of Physical Chemistry, 2007. **111**(17): p. 6281.
13. Frens, G., *Controlled Nucleation for the Regulation of the Particle Size in Monodisperse Gold Suspensions*. Nature Physical Sciences, 1973. **241**(105): p. 20-22.
  14. J. Kimling, M.M., B. Okenve, V. Kotaidis, H. Ballot, A. Plech, *Turkevich Method for Gold Nanoparticle Synthesis REvisited*. Journal of Physical Chemistry, 2006. **110**(32): p. 15700-15707.
  15. Jana, N.R., L. Gearheart, and C.J. Murphy, *Evidence for Seed-Mediated Nucleation in the Chemical Reduction of Gold Salts to Gold Nanoparticles*. Chemistry of Materials, 2001. **13**(7): p. 2313-2322.
  16. Burda, C., et al., *Chemistry and Properties of Nanocrystals of Different Shapes*. Chemical Reviews, 2005. **105**(4): p. 1025-1102.
  17. Cushing, B.L., V.L. Kolesnichenko, and C.J. O'Connor, *Recent Advances in the Liquid-Phase Syntheses of Inorganic Nanoparticles*. Chemical Reviews, 2004. **104**(9): p. 3893-3946.
  18. D. Fennell Evans, Joyce B. Evans, Radha Sen, and Gregory G. Warr, *A Comparison of Counterion Effects in Surfactant and Classical Colloid Systems*. Journal of Physical Chemistry, 1987. **92**: p. 784-790.
  19. Song Hi Lee, J.C.R., *Molecular dynamics simulation of ionic mobility. I Alkali metal cations in water at °25 C*. Journal of Chemical Physics, 1994. **101**(8).

## Appendix A

Figure 6 Data Collection: 0.175 mM Au was used for seed growth and 750 $\mu$ L samples were pulled from 100mL reaction volume at each time point and put on ice to stop reaction for disc centrifuge analysis.

Figure 7 Data Collection: For size distribution data, seeds were pH-adjusted to 7.3 with 1M NaOH before growth. 0.175 mM Au was used for seed growth. 750 $\mu$ L samples were withdrawn from reaction at the indicated intermediate time points and immediately put on ice to stop reaction. Samples were then analyzed with disc centrifugation. For TEM images, seeds were also pH-adjusted in the same manner and 1mL samples were put on ice at indicated time points. 0.150 mM Au was used for seed growth.

Figure 8 Data Collection: For all sizing data, seeds were grown with the desired citrate. They were then pH-adjusted to 7.3 with 1M LiOH, NaOH, or KOH depending on which type of citrate was used for particle growth, matching LiOH with Li<sub>3</sub>citrate, etc. 0.175 mM HAuCl<sub>4</sub> was added and then 750 $\mu$ L samples were withdrawn from reaction at the indicated intermediate time points and immediately put on ice to stop reaction. Samples were then analyzed with disc centrifugation.

Figure 9 Data Collection: Seeds were grown with lithium, sodium or potassium citrate and then pH-adjusted to 7.3 with 1M LiOH, NaOH or KOH depending on which type of citrate was used for synthesis. 0.175 mM of gold chloride was added to start the particle growth steps. The gold chlorides used were HAuCl<sub>4</sub>, LiAuCl<sub>4</sub>, NaAuCl<sub>4</sub> and KAuCl<sub>4</sub>. LiAuCl<sub>4</sub> was only used as the gold chloride when lithium citrate was used as the reducing agent and similarly for the other two alkali metal counterion gold chlorides. 750 $\mu$ L

samples were withdrawn from the reaction at indicated time points and pout on ice to stop the reaction. Samples were then analyzed in the disc centrifuge.

Figure 10 Data Collection: Same experimental set up as Figure 8 but pH adjustment before growth was 6.7 and 7.3.

Figure 11 Data Collection: Same experimental set up as Figure 10.

Figure 12 Data Collection: Same experimental set up as Figure 9 but pH adjustment before growth was 6.7.

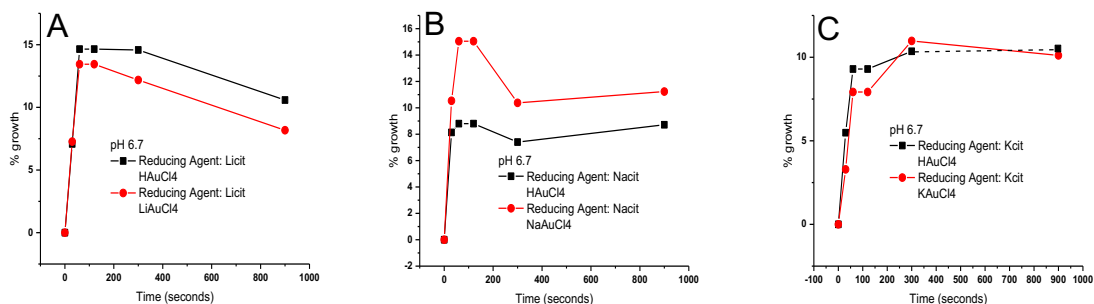


Figure 13: The three gold chloride counterions analyzed for the growth of seed-mediated gold nanoparticles were  $\text{Li}^+$ ,  $\text{Na}^+$ , and  $\text{K}^+$ . Each plot shows the comparison of  $\text{HAuCl}_4$  versus the different alkali metals as gold chloride counterions at pH 6.7. Plot (A) shows the comparison growth as a percentage for  $\text{HAuCl}_4$  and  $\text{LiAuCl}_4$ . Plot (B) shows the comparison growth as a percentage for  $\text{HAuCl}_4$  and  $\text{NaAuCl}_4$ . Plot (C) shows the comparison growth as a percentage for  $\text{HAuCl}_4$  and  $\text{KAuCl}_4$ . The plots show growth as a percentage increase in diameter of the particles versus time in seconds.

### Author's Biography

Andrew B. Closson was born in Hampden, Maine on August 31, 1993. He graduated from Hampden Academy in 2012. Majoring in Bioengineering, Andrew has a minor in nanotechnology and expects to graduate in December 2016. He is a member of the Tau Beta Pi engineering honors society. Upon graduation, Andrew plans to attend graduate school for Biomedical Engineering.